Symmetry analysis for film boiling of nanofluids on a vertical plate using a nonlinear approach

Andriy A. Avramenko, Igor V. Shevchuk, Shaaban Abdallah, D.G. Blinov, Souad Harmand, Andrii I. Tyrinov

Journal of Molecular Liquids 223 (2016) 156–164

Symmetry analysis for film boiling of nanofluids on a vertical plate using a nonlinear approach

A.A. Avramenko [a], I.V. Shevchuk [b,*], S. Abdallah [c], D.G. Blinov [a], S. Harmand [d], A.I. Tyrinov [a]

[a] Institute of Engineering Thermophysics, National Academy of Sciences, Kiev 03057, Ukraine
[b] MBtech Group GmbH & Co. KGaA, 70736 Fellbach-Schmiden, Germany
[c] Cincinnati University, OH 45221-0070, USA
[d] Université de Valenciennes et du Hainaut Cambrésis, TEMPO EA 4542, F-59313 Valenciennes, France

A B S T R A C T

This paper focuses on developing a self-similar model to be used in modeling of transport processes of heat, momentum and concentration in a nanofluid at its stable film boiling over a vertical surface. Novelty of the model consists in finding self-similar forms of variables and differential equations for a nanofluid via application of the Lie group theory. In the process of finding the self-similar forms, functional dependence of physical properties (viscosity, thermal conductivity and diffusion coefficient) on the nanoparticle concentration and temperature have been taken into account. As a result, novel self-similar functions for flow rate, enthalpy and nanoparticle concentration have been derived. The self-similar model proposed in the paper is universal since it does not involve any specific form of functional dependence of physical properties. The model incorporates also effects of the Brownian and thermophoretic diffusion. Six major non-dimensional parameters have been revealed, which stand for effects of the nanoparticles on heat transfer and fluid flow in the vapor film. They include the Schmidt number Sc; nanoparticle concentration ϕ_∞; normalized densities of the nanoparticles r_{pv} and r_{pL} (being dependent parameters); relative thermal conductivity of the nanoparticles κ and the complex parameter Ja/Pr. The subsequent simulations are based on the numerical solution of momentum, energy and mass transport equations in a self-similar form. It was shown that increased nanoparticle concentration enhances heat transfer.

1. Introduction

Adding nanoparticles to a pure fluid significantly increases heat transfer; an overview of the arising physical phenomena and their quantification is elucidated in the reviews of Wenhua et al. [1], Kakaç and Pramuanjaroenkij [2] and Buschmann [3]. A study of heat transport in suspensions of nanoparticles in nanofluids has been undertaken by Keblinski et al. [4]. During the last years, the number of investigations into heat transfer in nanofluids with phase transitions has significantly increased due to the perspective to use nanofluids e.g. for in quenching processes (Kim et al. [5]) and nuclear engineering (Bang et al. [6]). It has been noticed in many studies that at boiling of different nanofluids, HTC (or wall heat flux) has significantly increased, for instance, by up to 4 to 5 times in experiments of Rohsenow [7] at boiling of water with an addition of TiO_2 and Al_2O_3 nanoparticles. Nanoparticles of TiO_2, SiO_2, CeO_2, Al_2O_3, Au and ZnO added to water and ethylene glycol abruptly, by 170 to 200%, increased the CHF [5]. Analogous results for the HTC and the CHF in nanofluids were described in the works of Ramesh and Prabhu [8], Wang and Mijumdar [9] and Bang and Chang [10].

Heat transfer intensification was different in different investigations. In experiments of Ramesh and Prabhu [8] in nucleate boiling of CuO-water nanofluid, the HTC and the CHF increased together with the nanoparticle concentration. After the nanoparticle concentration reached 1%, the HTC passed over its maximum and began decreasing. In the experimental study of boiling of an Al_2O_3-water nanofluid performed by Bang and Chang [10], an increase in the nanoparticle concentration caused an increase in the CHF up to 32% over a horizontal and 13% over a vertical surface. However, Wang and Mijumdar [9] and Lotfi and Shafii [11] revealed heat transfer and CHF decrease at boiling in nanofluids. Bang et al. [6] attributed the aforementioned differences in the boiling curves to appearance of a nanoparticle layer on the heated wall. This layer is several microns thick and may change the contact angle (responsible for wettability of a solid surface by a liquid) and the number of nucleation cites. Simultaneously, the onset of a nanoparticle layer expedites heat conduction on the heating surface.

Experimental studies of the boiling processes in nanofluids have been intensively performed during the last several years. Heat transfer measurements in pool boiling of functionalized nanofluid at atmospheric and sub-atmospheric pressures done by Yang and Liu [12] demonstrated increased HTC as compared with pure water and almost no effect on the CHF. Experimental studies of Wen et al. [13] on nucleate

* Corresponding author.
E-mail address: igor.shevchuk@daad-alumni.de (I.V. Shevchuk).

DOI : 10.1016/j.molliq.2016.08.038

Nomenclature

A	parameter A, the relation between the mechanisms of the thermophoretic and Brownian diffusion, Eq. (30)
c	specific heat capacity
d_p	particle diameter
D_B	Brownian diffusion coefficient
D_T	thermophoretic diffusion coefficient
f	self-similar stream function
g	acceleration of gravity
G	mass flow rate through the vapor film
h	enthalpy
H	self-similar function of enthalpy
Ja_h, Ja	Jacoby numbers, Eqs. (27) and (34)
k	thermal conductivity of the vapor with nanoparticles
k_B	Boltzmann constant
Le	Lewis number
L_v	latent heat of vaporization
Nu	Nusselt number, Eq. (41)
Pr	Prandtl number
Sc	Schmidt number
T	temperature
u	streamwise velocity component
v	wall-normal velocity components
x, y	Cartesian coordinates

Greek symbols

α	heat transfer coefficient, Eq. (42)
δ	thickness of the vapor film
η	self-similar variable, Eq. (14)
Θ	dimensionless temperature, Eq. (30)
μ	dynamic viscosity
ρ	density
ϕ	nanoparticle concentration (volume fraction)
Φ	self-similar function of nanoparticle concentration

Subscripts

f	fluid
p	properties of nanoparticles
v	properties of the pure vapor
w	wall
∞	outer boundary of the condensation film

Acronyms

HTC	heat transfer coefficient
CHF	critical heat flux
3D	three-dimensional

boiling heat transfer with aqueous alumina nanofluids revealed that deposition of particles onto a heating smooth surface increased surface roughness resulting in increased nucleate boiling heat transfer, whereas geometry of a rough surface has not changed, which resulted in a similar boiling curve. Park et al. [14] investigated film boiling of Al_2O_3 nanofluids on a small (10 mm diameter) steel sphere and showed that presence of nanoparticles intensified vaporization at film boiling and diminishes heat flux. Nevertheless, the literature presents practically no data on the effect of nanoparticles on laminar film boiling over a vertical flat surface relevant to transport phenomena in biotechnology and food processing industry.

During the last years, numerous authors have undertaken theoretical studies of heat transfer in nanofluids. Thama et al. [15] modeled boundary layer flow of a nanofluid with the help of the Buongiorno-Darcy model and a finite-difference scheme. Effects of thermophoresis were studied theoretically by Eslamian and Saghir [16]. 3D transient model of a vapor chamber was developed by Hassan and Harmand [17], who studied effects of nanofluids on the performance of this vapor chamber. Altaç and Altun [18] performed a numerical study of steady-state developing flow and heat transfer of a nanofluid in a spiral tube coils using the FLUENT software. Li et al. [18] discussed the phenomenon of formation of a porous layer of deposited nanoparticles on the heated wall, which incurs much higher average nanoparticle concentration in the microlayer in comparison with the rest of the liquid. A novel heat flux partitioning model for nucleate boiling of nanofluids considering nanoparticle Brownian motion in a liquid microlayer enabled Li et al. [18] to model this phenomenon.

A new mathematic model was developed by Li et al. [19] to simulate nucleate pool boiling of nanofluids with account for Brownian motion of nanoparticles, active site density and the bubble departure diameter. The model of Li et al. [20] works in combination with two-fluid boiling model employed to simulate the nucleate pool boiling process.

Self-similar analysis as an analytical mathematical approach is currently widely used to model laminar and turbulent boundary layer flows over flat surfaces. This approach has been also employed for nanofluid flow by Avramenko et al. [21,22], whereas thermophysical properties of a nanofluid as a function of both nanoparticle concentration and temperature are included in the model. Here the symmetry analysis was used as a mathematical methodology to find out individually fitted self-similar variables and functions.

Koh [23] was apparently the first who proposed a self-similar approach for modeling stable film boiling of a pure one-phase liquid over a flat plate and derived a system of ordinary differential equations to be numerically solved for this purpose. Boundary-layer equations were simultaneously treated for liquid and vapor phases. Koh [23] showed that in boiling heat transfer the interfacial shear is an important parameter, which quite different from zero.

Avramenko et al. [24] developed analytical models of Bromley [25] and Ellion [26] used to simulate heat transfer at stable film boiling of a nanofluid film a vertical plate. The basic assumption of Avramenko et al. [24] was that the inertia force of the vapor film is negligibly small. The authors found six major non-dimensional parameters, which describe effects of the nanoparticles on heat transfer and fluid flow in the vapor film. It was shown that an increase in the nanoparticle concentration expedites the processes of momentum, mass and heat transfer.

The model of Avramenko et al. [24] has been also used in a series of other investigations. These works have been devoted to the study of heat transfer in film boiling of nanofluids [27] and magnetic nanofluids [28,29]. The model was implemented as a component part of the modeling approach based on numerical methods of simulations.

However, as it was shown by Koh [23], the assumption regarding vanishingly small influence of inertia force is valid only for the case where the parameter Ja/Pr is less than unity (a discussion and interpretation of this parameter is given below in the main body of the paper). With the increase in the parameter Ja/Pr, the role of inertia force also increases, which makes including it in the mathematical model and further calculations inevitable.

In view of the aforementioned, this article focuses on the study of heat transfer in film boiling of a nanofluid over a vertical surface with account for inertia force in the mathematical model. While considering the problems of heat transfer in nanofluids, one must take into account combined effects of the nanoparticle concentration on all thermophysical properties, because the HTC, being a function of thermal conductivity, is also subject to the influence of the flow structure, thickness of the condensation layer and other flow characteristics.

The model proposed in this investigation is an extension of the model suggested by Koh [23] to be applied for the study of heat transfer at film boiling over a vertical surface. This model includes the transport equation for the nanoparticle concentration taking into consideration heat transfer intensification due to the addition of nanoparticles plus the effects of mass transfer. Using the formulated model, one needs to search for the dimensionless parameters, which outline the effects of

nanoparticles on fluid flow, heat and mass transfer, in order to derive relations for velocity profiles, mass flow rate and heat transfer rate. Opposite to the most of the theoretical studies of nanofluid flow, our work considers in full effects of nanoparticles on the viscosity, thermal conductivity and density of the nanofluid.

Lie group theory will be employed to obtain self-similar forms of variables for the flow rate, enthalpy, nanoparticle concentration and transport equations.

Application of the theory of Lie groups will be used to find out self-similar forms of differential equations in the most general form taking into account any arbitrary dependence of physical properties (viscosity, thermal conductivity and diffusion coefficient) on the nanoparticle concentration and temperature. Therefore the finally derived equations are universal since they do not depend on the specific functional dependence of physical properties.

2. Mathematical model

The present study focuses on a problem of convective heat transfer between a vapor layer (or film) and a vertical flat wall kept at a constant temperature T_w (Fig. 1). In the chosen coordinate system, the x coordinate is aligned with the wall surface, the y coordinate is orthogonal to it, whereas the zero point of is located on the wall (Fig. 1). The vapor in the film moves upwards towards the larger x-values. The fluid surrounding the vapor film contains nanoparticles with concentration ϕ_∞. Here subscript w means conditions on the wall and subscript ∞ stands for conditions at the outer edge of the vapor layer. The vapor film has thickness δ, which is significantly smaller than the length of the wall, which backs up the boundary layer assumption used for modeling the film. The vapor, as well as the fluid temperature T_∞ at the outer boundary of the film $y = \delta$, are equal to the saturation temperature at a given pressure. The wall is heated more than the fluid: $T_w > T_\infty$.

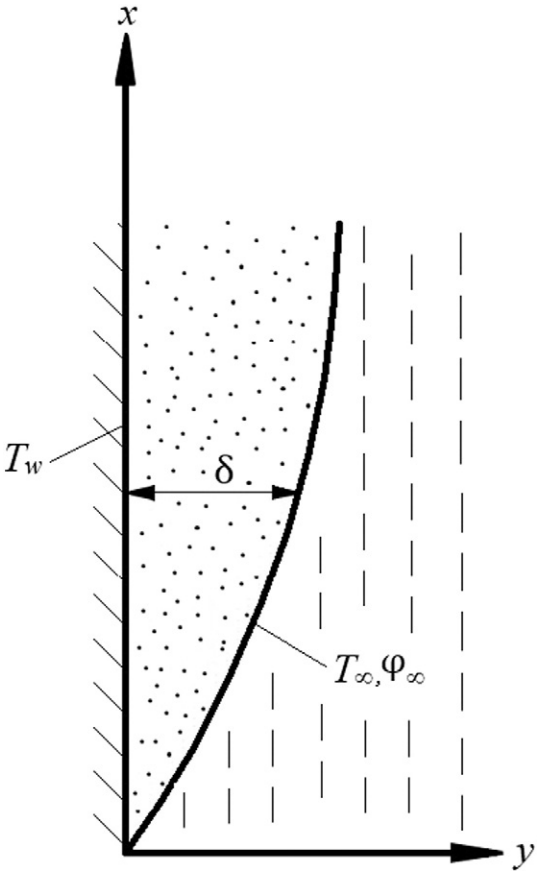

Fig. 1. Schematic of the modeled geometry.

The problem solution will be found given the following assumptions: vapor density is much smaller than fluid density; surface tension effects at the outer boundary of the vapor film, as well as fluid flow outside of the vapor film, can be ignored.

Based on these assumptions, fluid flow, heat and mass transfer in the vapor film with nanoparticles over a heated wall can be described by the following differential equations

$$\frac{\partial \rho u}{\partial x} + \frac{\partial \rho v}{\partial y} = 0 \tag{1}$$

$$\rho\left(u\frac{\partial u}{\partial x} + v\frac{\partial u}{\partial y}\right) = \frac{\partial}{\partial y}\left(\mu\frac{\partial u}{\partial y}\right) + g\rho_f \tag{2}$$

$$\rho\left(u\frac{\partial h}{\partial x} + v\frac{\partial h}{\partial y}\right) = \frac{\partial}{\partial y}\left(k\frac{\partial T}{\partial y}\right) + \rho_p c_p\left(D_B\frac{\partial \phi}{\partial y}\frac{\partial T}{\partial y} + \frac{D_T}{T}\frac{\partial T}{\partial y}\frac{\partial T}{\partial y}\right) \tag{3}$$

$$u\frac{\partial \phi}{\partial x} + v\frac{\partial \phi}{\partial y} = \frac{\partial}{\partial y}\left(D_B\frac{\partial \phi}{\partial y} + \frac{D_T}{T}\frac{\partial T}{\partial y}\right) \tag{4}$$

where u and v are streamwise and wall-normal velocity components (i.e. x- and y-components), respectively; ρ, μ and k are density, viscosity and thermal conductivity nanovapor; ρ_f is fluid density; ρ_p and c_p are density and specific heat capacity of the particles; $h = cT$ and c are enthalpy and specific heat capacity nanovapor; T is temperature; ϕ is nanoparticle volume fraction; D_B and D_T are Brownian diffusion coefficient and thermophoretic diffusion coefficient, respectively. Eqs. (1)–(4) are complemented with the following additional relations [30]

$$\mu = \frac{\mu_v}{(1-\phi)^{2.5}}, \quad D_B = \frac{k_B T}{3\pi\mu d_p}, \quad D_T = \beta\frac{\mu}{\rho}\phi \tag{5}$$

$$\begin{aligned} \rho &= (1-\phi)\rho_v + \phi\rho_p, \\ \rho c &= (1-\phi)(c\rho)_v + \phi(c\rho)_p, \\ \beta &= (1-\phi)\beta_v + \phi\beta_p \end{aligned} \tag{6}$$

$$k = k_v\left[\frac{k_p + 2k_v + 2\phi(k_v - k_f)}{k_p + 2k_v - \phi(k_v - k_f)}\right] \tag{7}$$

where subscripts v and p stand for vapor and particles, respectively; k_B is the Boltzmann constant, d_p is the particle diameter.

To solve Eqs. (1)–(4), the boundary conditions suggested by Ellion [26] will be applied here. These boundary conditions specify stationary fluid environment and have been also used as a limiting case in the investigations of Koh [23]

$$u = v = 0, \quad T = T_w, \quad \left(D_B\frac{d\phi}{dy}\right)_{y=0} = -\left(\frac{D_T}{T_\infty}\frac{dT}{dy}\right)_{y=0} \quad \text{at} \quad y = 0, \tag{8}$$

$$u = 0, \quad T = T_\infty, \quad \phi = \phi_\infty \quad \text{at} \quad y = \delta \tag{9}$$

The last relation in Eq. (8) outlines mathematically equality of the total flux of nanoparticles (Stefan's flow) on the wall at $y = 0$ due to the concentration gradient (the left-hand of the last Eq. (8)) to the total flux of nanoparticles incurred by the temperature gradient (the right-hand side of the last Eq. (8)) in line with suggestions of Lienhard IV and Lienhard V [31] and Baehr and Stephan [32].

Following Koh [23], a relation for the outer boundary of the vapor layer δ will be obtained from the mass balance

$$dG = k_\infty\left(\frac{dT}{dy}\right)_{y=\delta} dx \tag{10}$$

where

$$G = \int_0^{\delta} \rho u dy \tag{11}$$

is the mass flow rate in the vapor film, k_∞ is the thermal conductivity at $y = \delta$, and L_v is the latent heat of vaporization.

3. Symmetry and self-similar forms of equations

An advantage of self-similar solutions consists in the possibility to reduce the system of partial differential Eqs. (1)–(4) to ordinary differential equations. The mathematical methodology widely used for this purpose is symmetry analysis (i.e. the Lie group analysis). Symmetries of systems (1)–(4) can be derived with the help of the infinitesimal generator [33]

$$\mathrm{q} = \xi_1 \frac{\partial}{\partial x} + \xi_2 \frac{\partial}{\partial y} + \varphi_1 \frac{\partial}{\partial u} + \varphi_2 \frac{\partial}{\partial \mathrm{v}} + \varphi_3 \frac{\partial}{\partial T} + \varphi_4 \frac{\partial}{\partial \phi} + \zeta_1 \frac{\partial}{\partial \rho} + \zeta_2 \frac{\partial}{\partial \mu} + \zeta_3 \frac{\partial}{\partial D_B} + \zeta_4 \frac{\partial}{\partial D_T} + \zeta_5 \frac{\partial}{\partial c} + \zeta_6 \frac{\partial}{\partial k} \tag{12}$$

where equations for the coefficients $\xi_1, \xi_2, \varphi_1, \varphi_2, \varphi_3, \varphi_4, \zeta_1, \zeta_2, \zeta_3, \zeta_4, \zeta_5, \zeta_6$ are relegated to the appendix.

For two reasons, the most convenient symmetry to derive self-similar variables is the Lie sub-algebra $\tilde{\mathrm{q}}_6$ (Eq. (A22)). Firstly, in contrary to $\tilde{\mathrm{q}}_1$ that describes translation symmetry with respect to coordinates x and y, the symmetry $\tilde{\mathrm{q}}_6$ involves scaling with symmetry respect to coordinates x and y, which is useful at building up the self-similar forms. Secondly, the sub-algebra $\tilde{\mathrm{q}}_6$ is free from transformations with respect to T, φ, ρ, μ, D_B, D_T, c and k.

As the next step, symmetry (Eq. (A22)) should be corrected with account for any of the functional dependences $\rho = \rho(\varphi)$, $\mu = \mu(\varphi)$, $D_B = D_B(T)$, $D_T = D_T(\varphi)$, $c = c(\varphi)$, $k = k(\varphi)$. The resulting self-similar functions of these variables do not contain parametric variables, for example, a function of the coordinate x. The only self-similar functions containing parametric variable are those for $u(x, y)$ and $\mathrm{v}(x, y)$, because these velocity components are included into the infinitesimal generator (Eq. (A22)).

At first, let us find the self-similar variable η derived from Eq. (A22) using the equation

$$x \frac{\partial \eta}{\partial x} + \frac{1}{4} y \frac{\partial \eta}{\partial y} = 0 \tag{13}$$

Integration of Eq. (13) yields the following solution

$$\eta = y \sqrt[4]{\frac{g \rho_f \rho_v}{4 \mu_v^2 x}} \tag{14}$$

Parameter $g\rho_f\rho_v/\mu_v^2$ in Eq. (14) was used solely for the purpose of parameterization of the self-similar variable, whereas the coefficient 4 was involved in order to transform the variable (Eq. (14)) in the limiting case to the respective variable for pure vapor [23]. The present analysis of the self-similar forms is valid for the condition of $F_8 = 0$. The function F_8 describes transposition principle of Prandtl, see Oberlack [34], and can be involved in the analysis of flow over surfaces having variable geometrical form. We consider here a flat plate, which means that $F_8 = 0$.

At second, let us determine the self-similar function f from Eq. (A22) using the following relation

$$x \frac{\partial f'}{\partial x} + \frac{1}{2} u \frac{\partial f'}{\partial u} = 0 \tag{15}$$

Here derivative $f'(\eta)$ is used for the sake of convenience in integrating the continuity Eq. (1). Integration of Eq. (15) brings

$$\rho u = 2 \rho_\infty f'(\eta) \sqrt{g x \frac{\rho_f}{\rho_v}} \tag{16}$$

Keeping in mind that continuity equation includes variable density, it makes sense in Eq. (16) to use parameter $g\rho_f/\rho_v$ again solely for parameterization of the self-similar variable. The coefficient 2 was involved with the purpose to have an opportunity to reduce Eq. (16) to the conditions for pure vapor [23].

Integration of the continuity Eq. (1) with account for Eq. (16) yields

$$\rho \mathrm{v} = \sqrt[4]{\frac{g \rho_f}{4 x \rho_v}} \rho_\infty (f' \eta - 3 f) \tag{17}$$

Introducing self-similar functions for enthalpy and nanoparticle volume fraction

$$h = h_\infty H(\eta), \quad \phi = \Phi(\eta) \tag{18}$$

and substituting Eqs. (16), (17) and (18) into Eqs. (2), (3) and (4) results in derivation of a system of ordinary differential equations

$$M f''' + \left[3R(\phi_\infty) f + \left(M' - 2M \frac{R'}{R} \right) \Phi' \right] f'' + \left[\Phi'^2 \left(2M \left(\frac{R'}{R} \right)^2 - M' \frac{R'}{R} - M \frac{R''}{R} \right) - \left(3R_v(\phi_\infty) \Phi' + M \Phi'' \right) \frac{R'}{R} \right] f' - 2R(\phi_\infty) f'^2 + \frac{R}{R(\phi_\infty)} = 0 \tag{19}$$

$$K H'' + \left[3 \mathrm{Pr} \mathrm{RC} \frac{R(\phi_\infty)}{R} f + \left(\frac{1}{\mathrm{Le}} + K' + 2 \left(\left(\frac{D}{\mathrm{Le}} + K \right) \left(\frac{R'}{R} - \frac{RC'}{RC} \right) \right) \right) \Phi' \right] H' + \left[K \Phi'' \left(\frac{R'}{R} - \frac{RC'}{RC} \right) + \Phi'^2 \left(\frac{1}{\mathrm{Le}} \left(\frac{R'}{R} - \frac{RC'}{RC} + D \left(\left(\frac{R'}{R} \right)^2 - 2 \frac{R'}{R} \frac{RC'}{RC} + \frac{RC'^2}{RC^2} \right) \right) + K' \left(\frac{R'}{R} - \frac{RC'}{RC} \right) + K \left(2 \frac{RC'^2}{RC^2} - 2 \left(\frac{R'}{R} \right)^2 \frac{RC'^2}{RC^2} + \frac{R''}{R} - \frac{RC''}{RC} \right) \right) \right] H + \frac{D}{\mathrm{Le}} \frac{H'^2}{H} = 0 \tag{20}$$

$$\left[1 - \frac{RC}{RC'} \left(D + \frac{R'}{R} \right) \right] \Phi'' - \left[\frac{RC}{RC'} \frac{H'}{D_T} \left(\frac{D_T'}{H} + D_B' \right) + 3 \mathrm{Sc} \frac{R(\phi_\infty)}{R} \frac{RC}{RC'} f \right] \Phi' + \left[\frac{D_T'}{D_T} \left(1 - \frac{R'}{R} \frac{RC}{RC'} \right) + \frac{R'^2}{R^2} \frac{RC}{RC'} - \frac{RC'}{RC} - \frac{R''}{R} \frac{RC}{RC'} + \frac{RC''}{RC'} \right] \Phi'^2 + \frac{RC}{RC'} \left(\frac{H'^2}{H^2} - \frac{H''}{H} \right) = 0 \tag{21}$$

where

$$R(\phi) = (1 - \phi) + \phi r_{pv}, \quad RC(\phi) = (1 - \phi) + \phi \frac{\rho_p c_p}{\rho_v c_v},$$
$$M(\phi) = (1 - \phi)^{-2.5}, \quad K(\phi) = \frac{\kappa + 2 + 2\phi(\kappa - 1)}{\kappa + 2 - \phi(\kappa - 1)}, \quad r_{pv} = \frac{\rho_p}{\rho_v}, \quad \kappa = \frac{k_p}{k_v}$$
$$\mathrm{Pr} = \frac{\mu_v c_v}{k_v}, \quad \mathrm{Sc}[H(\eta)] = \frac{\mu_v}{\rho_v D_B}, \quad D = \frac{D_T}{D_B}, \quad \mathrm{Le}[H(\eta)] = \frac{\mathrm{Sc}[H(\eta)]}{\mathrm{Pr}} \frac{\rho_v c_v}{\rho_p c_p}. \tag{22}$$

In Eqs. (19), (20) and (21), primes in the functions f', H' and Φ' stand for derivatives with respect to η, primes in the functions R', RC', M', K' and D'_T stand for derivatives with respect to Φ, and primes in the functions D'_B mean derivatives with respect to H. It is worth pointing out that the Prandtl number here is constant, as it is based only on the properties of pure vapor.

Boundary conditions (8) and (9) can be re-written as

$$f = 0, \quad f' = 0, \quad H = \frac{h_w}{h_\infty}, \quad \frac{H'}{H} = \Phi' \left(\frac{RC'}{RC} - D \right) \quad \text{at} \quad \eta = 0, \tag{23}$$

$$f' = 0, \quad H = 1, \quad \Phi = \phi_\infty \quad \text{at} \quad \eta = \eta_\delta, \tag{24}$$

where

$$\eta_\delta = \delta \sqrt[4]{\frac{g\rho_f\rho_v}{4\mu_v^2 x}}. \tag{25}$$

In view of Eq. (11), one can derive from Eq. (10) the following relation for the outer boundary of the vapor layer

$$3f(\eta_\delta) = \frac{\mathrm{Ja}_h}{\mathrm{Pr}} \frac{K(\phi_\infty)}{RC(\phi_\infty)} \left[-H'(\eta_\delta) + \left(\frac{RC'(\phi_\infty)}{RC(\phi_\infty)} - \frac{R'(\phi_\infty)}{R(\phi_\infty)} \right) H'(\eta_\delta)\Phi'(\eta_\delta) \right], \tag{26}$$

where

$$\mathrm{Ja}_h = \frac{h_\infty}{L_v} \tag{27}$$

is the Jacoby number characterizing the ratio of the latent heat of vaporization and heat transferred by heat conduction and heat convection.

In the boundary conditions (23) an additional parameter h_w/h_∞ arises. To eliminate this parameter from the further consideration, one can replace enthalpy with the temperature in the energy Eq. (3) under fully justifiable assumption for the specific heat capacity of nanofluid to be constant. Other additional assumptions are $D_B = \text{const}$, $D_T = \text{const}$ and setting temperature to be constant equal to T_∞ in the denominators in the last terms of Eqs. (3) and (4) [30].

In view of the assumptions made above, partial differential equations, Eqs. (3) and (4), can be reduced to the self-similar form

$$K\Theta'' + \left(3R(\phi_\infty)\,\mathrm{Pr} f + \frac{\Phi'}{\mathrm{Le}} + K'\Phi' \right)\Theta' + \frac{A}{\mathrm{Le}}\Theta'^2 = 0 \tag{28}$$

$$\Phi'' + 3R(\phi_\infty)\frac{\mathrm{Sc}}{R} f\Phi' + A\Theta'' = 0 \tag{29}$$

where

$$\frac{T - T_w}{T_\infty - T_w} = \Theta(\eta), \qquad A = \frac{T_w - T_\infty}{T_\infty} D \tag{30}$$

System of Eqs. (19), (28) and (29) is to be complemented with the boundary conditions (8) and (9) re-written as

$$f = 0, \quad f' = 0, \quad \Theta = 1, \quad D\Theta' = -\Phi' \quad \text{at} \quad \eta = 0, \tag{31}$$

$$f' = 0, \quad \Theta = 0, \quad \Phi = \phi_\infty \quad \text{at} \quad \eta = \eta_\delta. \tag{32}$$

Based on this one can find the outer boundary of the vapor layer using the following equation

$$\frac{3f(\eta_\delta)}{-\Theta'(\eta_\delta)} = \frac{\mathrm{Ja}}{\mathrm{Pr}} \frac{K(\phi_\infty)}{R(\phi_\infty)}, \tag{33}$$

where

$$\mathrm{Ja} = \frac{c_v \Delta T}{L_v} \tag{34}$$

is re-written Jacoby number.

4. Results and discussion

Eqs. (19), (28) and (29) together with the boundary conditions (31) and (32) have been used for numerical simulations of heat and mass transfer and fluid flow in a film boiling of nanofluids on a vertical plate for wide range of variation of the parameters Sc, ϕ_∞, κ, r_{pv}, r_{pL} and complex Ja/Pr, where

$$r_{pL} = \frac{\rho_p}{\rho_L}, \tag{35}$$

and ρ_L is density of the pure liquid.

Simulations have been performed using "MATLAB" software and an in-house code written using programming language C++. The objective was to validate these two types of software against each other. To conclude, agreement between them was very good, with the deviations of the results from each other not exceeding 1%. The computational time of simulations increases together with the Schmidt (Lewis) number, which results from the increase in the stiffness of the system of differential equations.

At first, we have carried out computations to validate the numerical codes for the system of equations obtained by Koh [23] for a film of pure vapor (without nanoparticles) on a vertical wall. This system has the following form

$$f''' + 3ff'' - 2f'^2 + 1 = 0, \tag{36}$$

$$\Theta'' + 3\,\mathrm{Pr} f\Theta' = 0. \tag{37}$$

It is easy to ascertain that this system is a limiting case of the system of Eqs. (19), (28) and (29), when the terms describing properties of nanoparticles disappear for $\varphi = 0$. In this case, the boundary conditions (31) and (32) reduce to

$$f = 0, \quad f' = 0, \quad \Theta = 1 \quad at \quad \eta = 0, \tag{38}$$

$$f' = 0, \quad \Theta = 0, \quad \text{at} \quad \eta = \eta_\delta. \tag{39}$$

Calculations performed using Eqs. (36) and (37) with the boundary conditions (38) and (39) demonstrated almost complete agreement with the data of Koch [23]. Velocity profiles for Ja/Pr = 0.249, Ja/Pr = 1.2653, Ja/Pr = 4.2639 (Pr = 0.5) and Ja/Pr = 0.2598, Ja/Pr = 1.5375, Ja/Pr = 7.2145 (Pr = 1) fully coincide with the profiles shown in the work [23]. The data for the Nusselt number obtained in our calculations also showed very good agreement with the data of [23]. Thus, one can draw a conclusion about the correctness of the numerical codes used in our simulations.

Calculations based on the complete system of Eqs. (19), (29) and (29) for nanofluids have been performed for two cases: Ja/Pr = 0.1 and Ja/Pr = 7.5, i.e. for small and large values of the parameter Ja/Pr. The reason for this was that for small values of parameter Ja/Pr, as also indicated Koh [23], simulations taking into account inertial forces are close to calculations without inertial forces done by Bromley [25] and Ellion [26]. Ignoring inertial forces for large values of the parameter Ja/Pr causes significant errors in the results of calculations.

Calculations demonstrated that the addition of nanoparticles leads to emergence of a concentration boundary layer. Concentration profiles for different values of the Schmidt number are depicted in Fig. 2. In the vicinity of the wall, the magnitude of concentration level reduces, though rather moderately. Such a behavior of the concentration profile is caused by the interaction of mechanisms of the Brownian and thermophoretic diffusion. It is obvious that the increase in the Schmidt number results in the decrease in the thickness of the concentration layer. Consequently, for the large Schmidt numbers, the concentration on the wall is quite high, which entails heat transfer enhancement. Thus, the numerical results obtained in the present work confirm the finding of Bang et al. [6], who wrote about the presence of a thin (few microns thick) nanoparticle layer on the heated wall.

Results of the calculations for the normalized Nusselt number as a function of the parameters characterizing properties of the nanofluid are discussed below. The normalized Nusselt number was determined

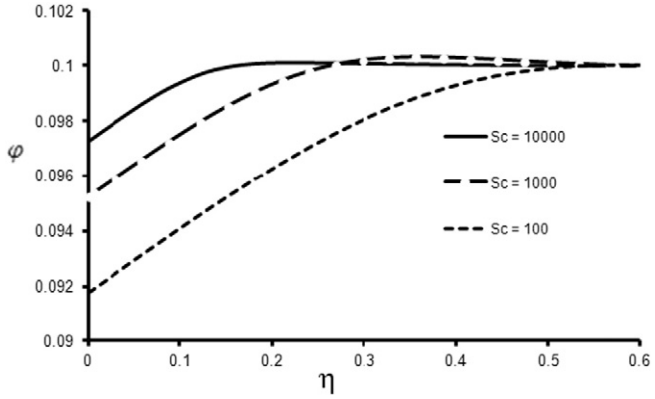

Fig. 2. Concenration boundary layer.

from the relation

$$\frac{\mathrm{Nu}}{\mathrm{Nu}_0} = K(\phi_w)\frac{[-\theta'(0)]}{[-\theta_0'(0)]}\sqrt[4]{\frac{\rho_f}{\rho_L}} = K(\phi_w)\frac{[-\theta'(0)]}{[-\theta_0'(0)]}\sqrt[4]{R_f(\phi_\infty)}, \tag{40}$$

where

$$\mathrm{Nu} = \frac{\alpha x}{k_v}, \quad \mathrm{Nu}_0 = \frac{\alpha_0 x}{k_v}, \tag{41}$$

$$\alpha = k_v K(\phi_w)\left(\frac{\partial T}{\partial y}\right)_{y=0}, \quad \alpha_0 = k_v\left(\frac{\partial T_0}{\partial y}\right)_{y=0}, \tag{42}$$

$$R_f(\phi) = (1-\phi) + \phi r_{pL}, \tag{43}$$

α is the heat transfer coefficient, subscript "0" means pure liquid (without nanoparticles).

Fig. 3 depicts the normalized Nusselt number as a function of the nanoparticle concentration ϕ_∞ for different values of the Schmidt number.

As one can see from Fig. 3, heat transfer rate increases monotonically with the increasing nanoparticle concentration and Schmidt number for both values of the parameter Ja/Pr. In both cases, the Schmidt number effect enhances with the increasing nanoparticle concentration.

The effect of the Schmidt number is caused by the formation of a concentration layer. As it was mentioned above (Fig. 2), for higher Schmidt numbers the nanoparticle concentration increases on the wall, which results in the heat transfer augmentation.

It should be pointed out that for Sc = 100 and Sc = 1000 an increase in the normalized Nusselt number is approximately the same for both values of the parameter Ja/Pr. However, an increase in the normalized Nusselt number for Sc = 10,000 is more noticeable for the smaller value of Ja/Pr = 0.1. It can be obviously attributed to the fact that for a pure fluid (without nanoparticles) at high values of parameter Ja/Pr the Nusselt number value Nu_0 is much higher than that for low values of Ja/Pr. Therefore the relative increase in the normalized Nusselt

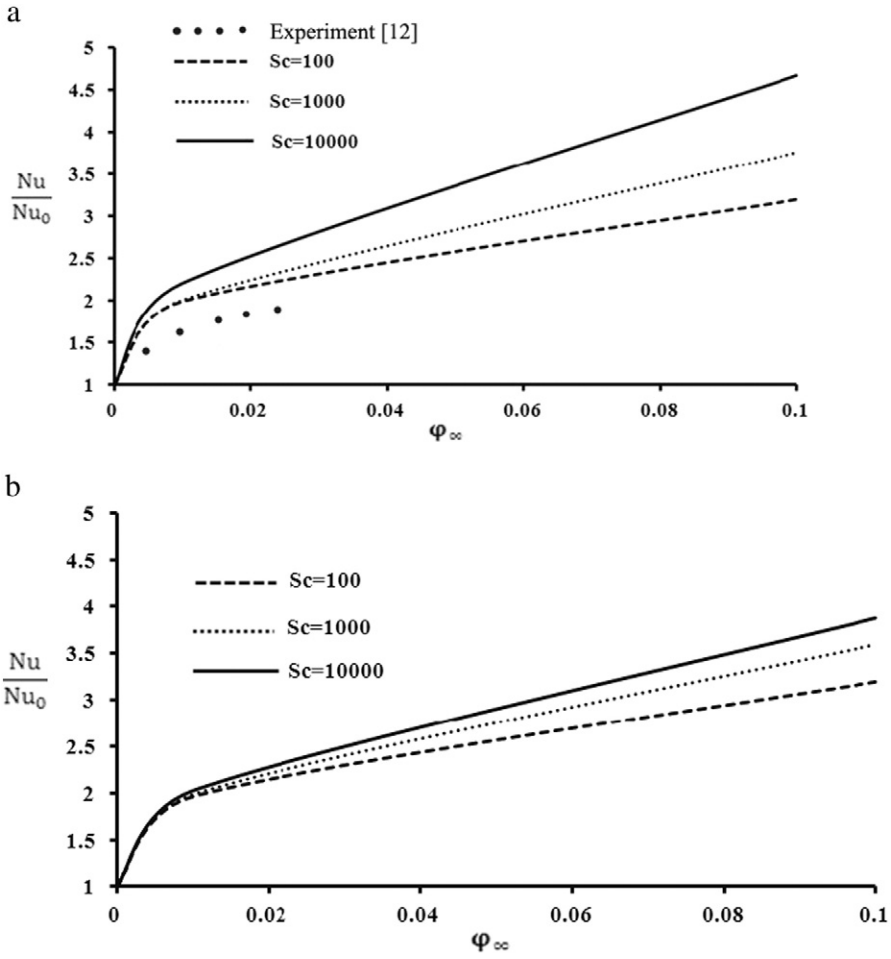

Fig. 3. Normalized Nusselt number as a function of the nanoparticle concentration for different values of the Schmidt number. a) Ja/Pr = 0.1, b) Ja/Pr = 7.5. Solid points: experimental data [12].

number is more noticeable namely at low values of Ja/Pr. It should be also pointed out that considering high Schmidt numbers is important for the nanofluid applications, because namely for typical nanofluids the Schmidt numbers attain significant values, for instance, Sc = 10,000 for water mixture with copper nanoparticles. Having compared results of the calculations in frames of the present study with the data of the work [24], where inertia forces and convective heat and mass transfer were not taken into account (similarly to work Bromley [25] and Ellion [26]), one can conclude that ignoring these effects leads to that the Schmidt number as a dimensionless parameter characterizing heat transfer does not arise in the solution at all. Thus, the approach ignoring inertia forces and convective heat and mass transfer is obviously disadvantageous.

For validation of our model and respective simulations, we selected experiments [12] for pool film boiling under the pressure of 7.4 KPa. Though these experiments have been performed in geometry different from that in Fig. 1, the physical trend describing effects of nanoparticles is expected to be analogous to that in our geometry. Experimental data [12] depicted in Fig. 3a lie lower than the theoretical curves; however, they demonstrate the same trend of the increased normalized Nusselt number for higher nanoparticle concentrations. As one can see from Fig. 3a, the theoretical model predicts a more pronounced effect of nanoparticles. Obviously, the reason for the difference in the theoretical and experimental data is caused by the different geometries, as well as the fact that the Buongiorno theory cannot take into account all peculiarities of heat transfer during boiling of nanofluids.

We have also derived a solution for $(Nu/Nu_0)_{Le\to\infty}$ for the case where terms including the Lewis number were omitted from Eq. (28). The purpose of the comparative analysis was to look in detail into the significance of different terms responsible for the effect of the Lewis number, which is of great importance for nanofluids. This analysis has shown that ignoring the aforementioned terms affects very little the results of computations even for medium and high Schmidt numbers.

Fig. 4 depicts variation of the normalized Nusselt number as a function of nanoparticle concentration for different values of nanoparticle density. One can conclude from here that an increase in the relative density of nanoparticles results in heat transfer enhancement. Again, as in Fig. 3, the increase in the normalized Nusselt number is more significant for smaller values of the parameter Ja/Pr = 0.1.

It can be also pointed out that the density effect for large nanoparticle concentration ($\phi_\infty \to 0.1$) is more pronounced at larger values of the parameter Ja/Pr = 7.5.

Comparisons of the present calculations with the data of the model that ignored inertia forces and convective heat and mass transfer [24] demonstrate approximately the same rate of increase of the normalized Nusselt number (see [24]). This enables drawing a conclusion that the model neglecting inertia forces and convective heat and mass transfer can be used for predictions of the normalized Nusselt number.

Fig. 5 describes the effect of the normalized thermal conductivity of nanoparticles, which is characterized by the parameter κ, on the normalized Nusselt number for different values of the nanoparticles concentration ϕ_∞.

As in both previous cases discussed above, this effect is somewhat stronger at smaller value of the parameter Ja/Pr = 0.1. It is also interesting to note the fact that for $\kappa > 10$ the further increase in the thermal conductivity of nanoparticles does not cause any significant increase in the heat transfer coefficient. For $\kappa > 10$, the curve $Nu/Nu_0 = Nu/Nu_0(\kappa)$ asymptotically flattens to a horizontal line. A similar effect was also observed in the model neglecting inertia forces and convective heat and mass transfer (see [24]).

Effects of the parameter A on the normalized Nusselt number were also investigated for two values of the Schmidt number (Sc = 100, Sc = 1000). Computations demonstrated that the influence of the parameter A on Nu/Nu_0 is weak. An increase in the parameter A by 60 times (from 0.01 to 0.6) results in the decrease in Nu/Nu_0 by only 4%.

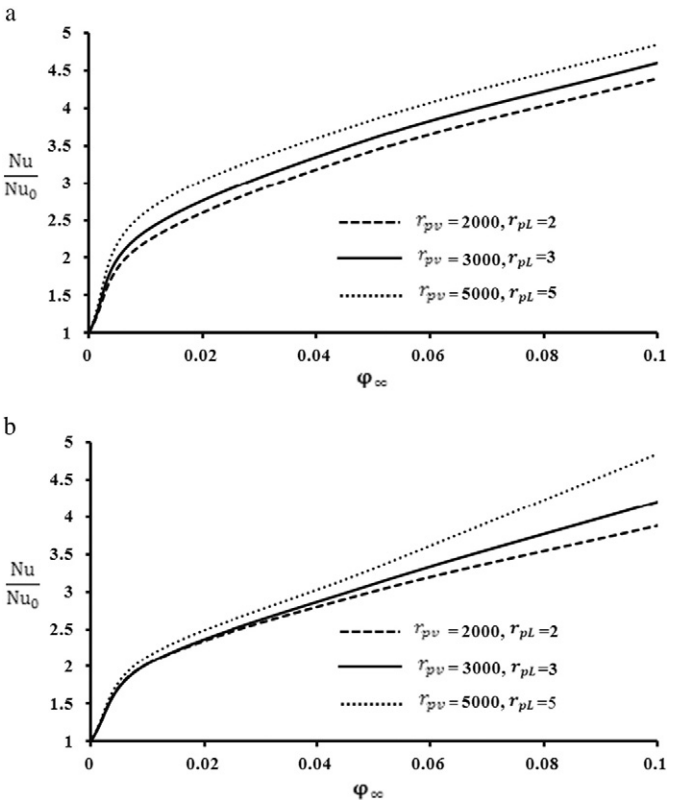

Fig. 4. Normalized Nusselt number as a function of the nanoparticle concentration for different nanoparticle density. a) Ja/Pr = 0.1, b) Ja/Pr = 7.5.

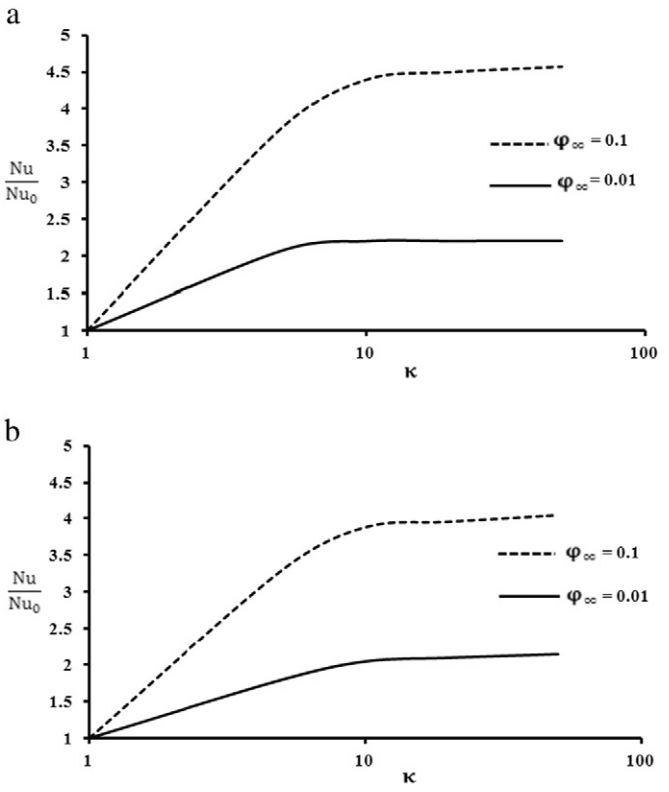

Fig. 5. Normalized Nusselt number as a function of the normalized thermal conductivity of nanoparticles for different values of nanoparticle concentration. a) Ja/Pr = 0.1, b) Ja/Pr = 7.5.

5. Conclusions

Using symmetry properties of the model of a two-component fluid, self-similar equations were derived to model heat transfer in film boiling of a nanofluid over a vertical flat wall. Self-similar system of ordinary differential equations was integrated numerically.

Physical novelty of the model proposed in our paper as compared to the film boiling problem studied by Koh [23] consists in adding an equation for nanoparticle concentration, which accounts for the heat transfer enhancement at the expense of the nanoparticles, as well as effects of mass transfer. The model takes also into consideration the Brownian and thermophoretic diffusion mechanisms, together with the nanoparticle concentration effects on the fluid properties. *Mathematical novelty* of the model consists in obtaining new self-similar forms of functions for flow rate, enthalpy, nanoparticle concentration and for the system of differential equations on the basis of the Lie group technique.

Self-similar form of differential equations have been obtained in the most general forms taking into account arbitrary dependence of physical properties (viscosity, thermal conductivity and diffusion coefficient) on the nanoparticle concentration and temperature. Therefore these equations are universal, whereas their form does not depend on the specific functional dependence of physical properties.

As it was demonstrated in the present work, fluid flow and heat transfer are affected by six non-dimensional parameters: Schmidt number Sc; nanoparticle concentration ϕ_∞; normalized densities of the nanoparticles r_{pv} and r_{pL} (which are not independent parameters); relative thermal conductivity of the nanoparticles κ and the complex parameter Ja/Pr.

Heat transfer rate grows monotonically with increasing nanoparticle concentration and Schmidt number for small (0.1) and large values (7.5) of the parameter Ja/Pr. It was also demonstrated that the Schmidt number arises as a result of the solution and characterizes heat transfer only in the case where inertia forces and convective heat mass transfer are taken into account. Numerical simulations have shown that ignoring terms including the Lewis number affects very little the results of computations even for medium and high Schmidt numbers.

An increase in the parameters r_{pv}, r_{pL} and κ leads to heat transfer enhancement. At $\kappa > 10$, the further increase in thermal conductivity of nanoparticles does not cause any significant increase in the heat transfer coefficient. The effect on heat transfer is somewhat stronger at the smaller value of the parameter Ja/Pr $= 0.1$.

Practical value of the present investigation consists in that the proposed self-similar model has universal character, because it does not depend on the specific form of the functional dependences of physical properties on the temperature and nanoparticle concentration. This means that this model can be used with arbitrary functional dependences for these functions.

Appendix A

To find symmetries of the system of partial differential Eqs. (1)–(4) (i.e. coefficients $\xi_1,\xi_2,\varphi_1,\varphi_2,\varphi_3,\varphi_4,\zeta_1,\zeta_2,\zeta_3,\zeta_4,\zeta_5,\zeta_6$), the following condition should be used

$$\mathrm{pr}^{(2)}\mathrm{q}(\Delta) = 0, \tag{A1}$$

where $\mathrm{pr}^{(2)}\mathrm{q}(\Delta)$ is the second prolongation of the infinitesimal generator (Eq. (14)), the symbol Δ means the system of partial differential Eqs. (1)–(4).

The second prolongation of the infinitesimal generator q (Eq. (14)) is constructed according to the following expression

$$\begin{aligned}\mathrm{pr}^{(2)}\mathrm{q} = \mathrm{q} &+ \varphi_1^x\frac{\partial}{\partial u_x} + \varphi_1^y\frac{\partial}{\partial u_y} + \varphi_1^{yy}\frac{\partial}{\partial u_{yy}} + \varphi_2^y\frac{\partial}{\partial \mathrm{v}_y} + \varphi_3^x\frac{\partial}{\partial T_x}\\ &+\varphi_3^y\frac{\partial}{\partial T_y} + \varphi_3^{yy}\frac{\partial}{\partial T_{yy}} + \varphi_4^x\frac{\partial}{\partial \phi_x} + \varphi_4^y\frac{\partial}{\partial \phi_y} + \varphi_4^{yy}\frac{\partial}{\partial \phi_{yy}},\end{aligned} \tag{A2}$$

where the subscripts of u, v, T and φ represent the partial derivatives with respect to the appropriate variables. The coefficients $\phi_1^x,\phi_1^y,\phi_1^{yy},\phi_2^y,\phi_3^x,\phi_3^y,\phi_3^{yy},\phi_4^x,\phi_4^y,\phi_4^{yy}$ are functions of $\xi_1,\xi_2,\phi_1,\phi_2,\phi_3,\phi_4,\zeta_1,\zeta_2,\zeta_3,\zeta_4,\zeta_5,\zeta_6$, u, v, T and φ and their derivatives with respect to x and y.

The application of the operator $\mathrm{pr}^{(2)}\mathrm{q}$ (Eq. (A2)) to each equation of systems (8)–(11) (according to condition (A1)) results in four equations. These equations contain monomials with different combinations of derivatives of u, v, T and φ. Then the coefficients of monomials containing identical combinations of the derivatives of u, v, T and φ are equated. As a result, one has a system of partial differential equations with respect to the $\xi_1,\xi_2,\varphi_1,\varphi_2,\varphi_3,\varphi_4,\zeta_1,\zeta_2,\zeta_3,\zeta_4,\zeta_5,\zeta_6$. The solution of this system consists of five symmetries (five Lie sub-algebras). After further transformations, the Lie algebra of the systems (1)–(4) can be finally presented as

$$\mathrm{q}_1 = \frac{\partial}{\partial x} + F_1(x)\frac{\partial}{\partial y} + \frac{dF_1(x)}{dx}u\frac{\partial}{\partial \mathrm{v}}, \tag{A3}$$

$$\mathrm{q}_2 = F_2(x)\frac{\partial}{\partial y} + \frac{dF_2(x)}{dx}u\frac{\partial}{\partial \mathrm{v}} + \frac{\partial}{\partial \phi}, \tag{A4}$$

$$\mathrm{q}_3 = F_3(x)\frac{\partial}{\partial y} + \frac{dF_3(x)}{dx}u\frac{\partial}{\partial \mathrm{v}} + \frac{1}{T}\frac{\partial}{\partial c}, \tag{A5}$$

$$\mathrm{q}_4 = F_4(x)\frac{\partial}{\partial y} + \frac{dF_4(x)}{dx}u\frac{\partial}{\partial \mathrm{v}} + \phi\frac{\partial}{\partial \phi} + D_T\frac{\partial}{\partial D_T} + c\frac{\partial}{\partial c} + k\frac{\partial}{\partial k}, \tag{A6}$$

$$\begin{aligned}\mathrm{q}_5 = F_5(x)\frac{\partial}{\partial y} + u\frac{\partial}{\partial u} + \left(\frac{dF_5(x)}{dx}u + \mathrm{v}\right)\frac{\partial}{\partial \mathrm{v}} - 2\rho\frac{\partial}{\partial \rho} - \mu\frac{\partial}{\partial \mu} + D_B\frac{\partial}{\partial D_B}\\ + D_T\frac{\partial}{\partial D_T} + 2c\frac{\partial}{\partial c} + k\frac{\partial}{\partial k},\end{aligned} \tag{A7}$$

$$\begin{aligned}\mathrm{q}_6 = x\frac{\partial}{\partial x} + F_6(x)\frac{\partial}{\partial y} + \left(\frac{dF_6(x)}{dx}u - \mathrm{v}\right)\frac{\partial}{\partial \mathrm{v}}\\ + \rho\frac{\partial}{\partial \rho} - D_B\frac{\partial}{\partial D_B} - D_T\frac{\partial}{\partial D_T} - c\frac{\partial}{\partial c} - k\frac{\partial}{\partial k},\end{aligned} \tag{A8}$$

$$\begin{aligned}\mathrm{q}_7 = (y + F_7(x))\frac{\partial}{\partial y} + \left(\frac{dF_7(x)}{dx}u + \mathrm{v}\right)\frac{\partial}{\partial \mathrm{v}} + 2\mu\frac{\partial}{\partial \mu} + 2D_B\frac{\partial}{\partial D_B}\\ + 2D_T\frac{\partial}{\partial D_T} + 2k\frac{\partial}{\partial k},\end{aligned} \tag{A9}$$

$$\mathrm{q}_8 = x\frac{\partial}{\partial x} + \left(\frac{1}{4}y + F_8(x)\right)\frac{\partial}{\partial y} + \frac{1}{2}u\frac{\partial}{\partial u} + \left(\frac{dF_8(x)}{dx}u - \frac{1}{4}\mathrm{v}\right)\frac{\partial}{\partial \mathrm{v}}, \tag{A10}$$

where $F_1(x)$, …, $F_8(x)$ are arbitrary smooth functions.

Let us construct an optimal system of the Lie sub-algebras. To remind (see the work [30]) that an optimal system is a list of the Lie subalgebras where every Lie subalgebra of the total Lie algebra is equivalent to a unique item in the list under some element of the adjoint representation

$$\tilde{\mathrm{q}} = \mathrm{Ad}H(\mathrm{q}), \tag{A11}$$

where Ad H is the adjoint representation of the underlying Lie group. This adjoint representation can be reconstructed by two ways. At first, it can be done by integrating the system of the linear ordinary differential equations

$$\frac{d\tilde{\mathrm{q}}}{d\varepsilon} = [\tilde{\mathrm{q}}, \mathrm{q}], \quad \tilde{\mathrm{q}}(0) = \tilde{\mathrm{q}}_0 \tag{A12}$$

with the solution

$$\tilde{\mathrm{q}}(\varepsilon) = \mathrm{Ad}(\exp(\varepsilon\mathrm{q}))\tilde{\mathrm{q}}_0. \tag{A13}$$

Another way is applying the Lie series

$$\mathrm{Ad}(\exp(\varepsilon \mathrm{q}))\tilde{\mathrm{q}}_0 = \tilde{\mathrm{q}}_0 - \varepsilon[\mathrm{q}, \tilde{\mathrm{q}}_0] + \frac{\varepsilon^2}{2}[\mathrm{q}, [\mathrm{q}, \tilde{\mathrm{q}}_0]] - \ldots. \tag{A14}$$

In Eqs. (A12)–(A15) $[\tilde{\mathrm{q}}, \mathrm{q}]$ is the Lie bracket

$$[\tilde{\mathrm{q}}, \mathrm{q}]F = \tilde{\mathrm{q}}(\mathrm{q}(F)) - \mathrm{q}(\tilde{\mathrm{q}}(F)), \tag{A15}$$

F is the smooth function, ε is the infinitesimal transformation parameter,

$$H(F) = \exp(\varepsilon \mathrm{q})F \tag{A16}$$

is the exponentiation of the vector field, i.e. the group transformation.

To construct an optimal system of the Lie sub-algebras, it is necessary to simplify the coefficients a_i of the non-zero vector

$$\mathrm{q} = \sum_{i=1}^{8} a_i \mathrm{q}_i, \tag{A17}$$

through judicious applications of the adjoint representations. Procedure of this mathematical operation is described in detail by Olver [30]. Applying this procedure to Eqs. (A3)–(A10) allows finding an optimal system of one-dimensional Lie sub-algebras, which has following form

$$\tilde{\mathrm{q}}_1 = \mathrm{q}_1, \tag{A18}$$

$$\tilde{\mathrm{q}}_2 = \mathrm{q}_2, \tag{A19}$$

$$\tilde{\mathrm{q}}_3 = \mathrm{q}_3, \tag{A20}$$

$$\tilde{\mathrm{q}}_4 = \mathrm{q}_4, \tag{A20}$$

$$\tilde{\mathrm{q}}_5 = \mathrm{q}_6 + C\mathrm{q}_7, \tag{A21}$$

$$\tilde{\mathrm{q}}_6 = \mathrm{q}_8, \tag{A22}$$

where C is an arbitrary constant.

References

[1] Y. Wenhua, D.M. France, J.L. Routbort, S.U.S. Choi, Review and comparison of nanofluid thermal conductivity and heat transfer enhancements, Heat Transfer Eng. 29 (2008) 432–460.
[2] S. Kakac, A. Pramuanjaroenkij, Review of convective heat transfer enhancement with nanofluids, Int. J. Heat Mass Transfer 52 (2009) 3187–3196.
[3] M.H. Buschmann, Nanofluids in thermosyphons and heat pipes: Overview of recent experiments and modelling approaches, Int. J. Therm. Sci. 72 (2013) 1–17.
[4] P. Keblinski, S.R. Phillpot, S.U.S. Choi, J.A. Eastman, Mechanisms of heat flow in suspensions of nano-sized particles (nanofluids), Int. J. Heat Mass Transfer 45 (2002) 855–863.
[5] H. Kim, G. DeWitt, T. McKrell, J. Buongiorno, L.W. Hu, On the quenching of steel and zircaloy spheres in water-based nanofluids with aluminia, silica and diamond nanoparticles, Int. J. Multiphase Flow 35 (2009) 427–438.
[6] I.C. Bang, J. Buongiorno, L.W. Yu, H. Wang, Measurement of key pool boiling parameters in nanofluids for nuclear applications, J. Power Energy Systems 2 (2008) 340–351.
[7] W.M. Rohsenow, A method of correlating heat transfer data for surface boiling liquids, Transactions of ASME 74 (1952) 969–979.
[8] G. Ramesh, N.K. Prabhu, Review of thermo-physical properties, wetting and heat transfer characteristics of nanofluids and their applicability in industrial quench heat treatment, Nanoscale Research Letters 334 (2011) 1–15.
[9] X.Q. Wang, A.S. Mujumdar, Heat transfer characteristics of nanofluids: a review, Int. J. Thermal Sci. 46 (2007) 1–19.
[10] I.S. Bang, S.H. Chang, Boiling heat transfer performance and phenomena of Al_2O_3–water nanofluids from a plain surface in a pool, Int. J. Heat Mass Transf. 48 (2005) 2420–2428.
[11] H. Lotfi, M.B. Shafii, Boiling heat transfer on a high temperature silver sphere in nanofluid, Int. J. Thermal Sci. 48 (2009) 2215–2220.
[12] X.F. Yang, Z.H. Liu, Pool boiling heat transfer of functionalized nanofluid under subatmospheric pressures, Int. J. Thermal Sci. 50 (2011) 2402–2412.
[13] D. Wen, M. Corr, X. Hu, G. Lin, Boiling heat transfer of nanofluids: the effect of heating surface modification, Int. J. Thermal Sci. 50 (2011) 480–485.
[14] H.S. Park, D. Shiferaw, B.R. Sehdal, D.K. Kim, M. Muhammed, Film boiling heat transfer on a high temperature sphere in nanofluid, ASME 2004 Heat Transf./Fluids Eng. Summer Conf. (Charlotte, NC, USA), 4, 2004, pp. 469–476.
[15] L. Thama, R. Nazar, I. Pop, Mixed convection flow from a horizontal circular cylinder embedded in a porous medium filled by a nanofluid: Buongiorno-Darcy model, Int. J. Thermal Sci. 84 (2014) 21–33.
[16] M. Eslamian, M.Z. Saghir, On thermophoresis modeling in inert nanofluids, Int. J. Thermal Sci. 80 (2014) 58–64.
[17] H. Hassan, S. Harmand, 3D transient model of vapour chamber: effect of nanofluids on its performance, Appl. Therm. Engineering 51 (2013) 1191–1201.
[18] Z. Altaç, Ö. Altun, Hydrodynamically and thermally developing laminar flow in spiral coil tubes, Int. J. Thermal Sci. 77 (2014) 96–107.
[19] X. Li, Y. Yuan, J. Tu, A theoretical model for nucleate boiling of nanofluids considering the nanoparticle Brownian motion in liquid microlayer, Int. J. Heat Mass Transf. 91 (2015) 467–476.
[20] K. Li, X.D. Li, J.Y. Tu, H.G. Wang, A mathematic model considering the effect of Brownian motion for subcooled nucleate pool boiling of dilute nanofluids Int, J. Heat Mass Transf. 84 (2015) 46–53.
[21] A.A. Avramenko, D.G. Blinov, I.V. Shevchuk, Self-similar analysis of fluid flow and heat-mass transfer of nanofluids in boundary layer, Phys. Fluids 23 (2011) 082002.
[22] A.A. Avramenko, D.G. Blinov, I.V. Shevchuk, A.V. Kuznetsov, Symmetry analysis and self-similar forms of fluid flow and heat-mass transfer in turbulent boundary layer flow of a nanofluid, Phys. Fluids 24 (2012) 092003.
[23] J.C.Y. Koh, Analysis of film boiling on vertical surfaces, ASME J. Heat Transfer (1962) 55–62.
[24] A.A. Avramenko, I.V. Shevchuk, A.I. Tyrinov, D.G. Blinov, Heat transfer in stable film boiling of a nanofluid over a vertical surface, Int. J. Thermal Sci. 92 (2015) 106–118.
[25] L.A. Bromley, Heat transfer in stable film boiling, Chem. Eng. Prog. 46 (1950) 211–227.
[26] M.E. Ellion, A study of the mechanism of boiling heat transfer, Jet Prop. Lab. Memo, 20, CIT 1954, pp. 1–88.
[27] A. Malvandi, S. Heysiattalab, D.D. Ganji, Thermophoresis and Brownian motion effects on heat transfer enhancement at film boiling of nanofluids over a vertical cylinder, J. Molecular Liquids 216 (2016) 503–509.
[28] A. Malvandi, Anisotropic behavior of magnetic nanofluids (MNFs) at film boiling over a vertical cylinder in presence of a uniform variable-directional magnetic field, Powder Technol. 294 (2016) 307–314.
[29] A. Malvandi, Film boiling of magnetic nanofluids (MNFs) over a vertical plate in presence of a uniform variable-directional magnetic field J, Magnetism and Magnetic Materials 406 (2016) 95–102.
[30] J. Buongiorno, Convective transport in nanofluids, ASME J. Heat Transfer 128 (2006) 240–250.
[31] J.H. Lienhard IV, J.H. Lienhard V, A Heat Transfer Textbook, third ed. Phlogiston Press, Cambridge Massachusetts, 2003.
[32] H.D. Baehr, K. Stephan, Heat and Mass Transfer, Second, Revised ed. Springer Verlag, Berlin, Heidelberg, 2006.
[33] P. Olver, Applications of Lie Groups to Differential Equations, Springer, New York, 1985.
[34] M. Oberlack, Asymptotic expansion, symmetry groups, and invariant solutions of laminar and turbulent wall-bounded flows, ZAMM 80 (2000) 791–800.